organics

MDPI

Article

Synthesis and Properties of 3,8-Diaryl-2*H*-cyclohepta[*b*]furan-2-ones

Taku Shoji [1,*], Daichi Ando [2], Masayuki Iwabuchi [1], Tetsuo Okujima [3], Ryuta Sekiguchi [4] and Shunji Ito [4]

[1] Department of Chemical Biology and Applied Chemistry, College of Engineering, Nihon University, Koriyama 963-8642, Fukushima, Japan
[2] Department of Material Science, Graduate School of Science and Technology, Shinshu University, Matsumoto 390-8621, Nagano, Japan
[3] Graduate School of Science and Engineering, Ehime University, Matsuyama 790-8577, Ehime, Japan; okujima.tetsuo.mu@ehime-u.ac.jp
[4] Graduate School of Science and Technology, Hirosaki University, Hirosaki 036-8561, Aomori, Japan; rsekiguchi@hirosaki-u.ac.jp (R.S.); itsnj@hirosaki-u.ac.jp (S.I.)
* Correspondence: shoji.taku@nihon-u.ac.jp; Tel.: +81-24-956-8808

Abstract: Synthesis of 3,8-diaryl-2*H*-cyclohepta[*b*]furan-2-ones was accomplished by the one-pot procedure involving sequential iodation and Suzuki–Miyaura coupling reactions. The optical and structural characteristics of 3,8-diaryl-2*H*-cyclohepta[*b*]furan-2-ones prepared were scrutinized using UV/Vis spectroscopy, theoretical calculations, and single-crystal X-ray crystallography. The redox properties of the compounds were also evaluated through cyclic voltammetry (CV) and differential pulse voltammetry (DPV). The findings reveal that the introduction of aryl groups at both the 3- and 8-positions significantly influences the electronic properties of the CHFs, resulting in distinct optical and electrochemical characteristics.

Keywords: 2*H*-cyclohepta[*b*]furan-2-ones; Suzuki–Miyaura coupling; single-crystal X-ray analysis

Citation: Shoji, T.; Ando, D.; Iwabuchi, M.; Okujima, T.; Sekiguchi, R.; Ito, S. Synthesis and Properties of 3,8-Diaryl-2*H*-cyclohepta[*b*]furan-2-ones. *Organics* **2024**, *5*, 252–262. https://doi.org/10.3390/org5030013

Academic Editor: Wim Dehaen

Received: 13 June 2024
Revised: 18 July 2024
Accepted: 29 July 2024
Published: 1 August 2024

1. Introduction

2*H*-Cyclohepta[*b*]furan-2-one (CHF) is recognized as one of the heteroazulenes [1], and its functionalized derivatives are known to exhibit inotropic character [2]. In their utilization of these derivatives, Ando et al. have demonstrated that CHFs can be used as starting materials for the total synthesis of natural products [3–5]. On the other hand, Nitta and co-workers have reported the synthesis and properties of methylium or tropylium ions connected with CHF [6–10]. As a result, these ions were found to be highly stable and to exhibit an absorption band with a large molar absorption coefficient in the visible region of the UV-visible absorption spectrum. The CHFs can also be effectively converted to azulene derivatives through reactions with olefins [11–13] and reactive intermediates, such as enamines [14–18], silyl enol ether [19], and active methylene compounds [20]. Although numerous methods for the conversion of CHFs to azulene derivatives have been documented, the modification method of CHF itself has not been extensively explored. Over the past decade, we have made strides in the electrophilic substitution [21–23] and cross-coupling reactions [24–26] of CHFs, primarily targeting the highly reactive 3-position (Figure 1).

Nevertheless, the synthesis of CHF derivatives featuring functional groups other than alkyl ones at the seven-membered ring has been limited. In this regard, we have developed a novel synthetic pathway to 8-aryl-CHFs by Suzuki–Miyaura coupling of 8-trifluoromethanesulfonyl-CHF obtained by the reaction of 8-hydroxy-CHF with trifluoromethanesulfonic anhydride [27]. In our previous work, we reported the first synthesis of 8-aryl-CHFs **2a**–**2c** by Suzuki–Miyaura coupling of triflate **1**, which was derived from the 8-hydroxy-CHF precursor. This method is innovative for its ability to introduce an aryl group at the difficult 8-position, which is not easily established using traditional methods.

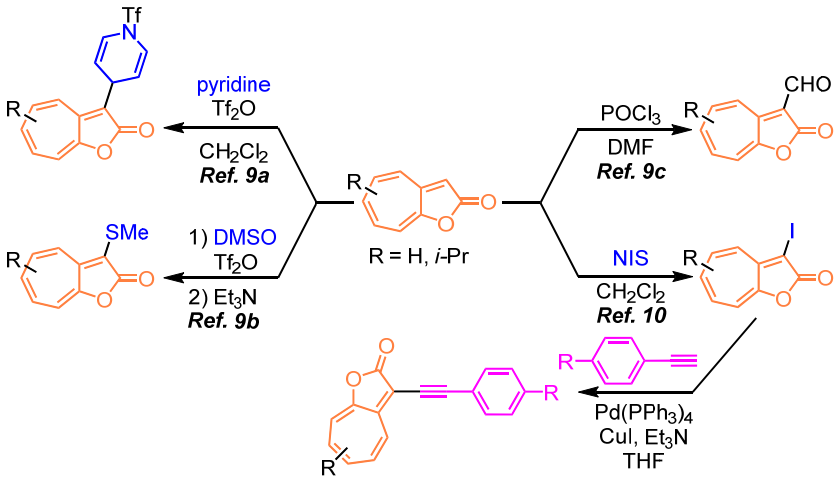

Figure 1. Overview of electrophilic substitution and cross-coupling reactions of CHF derivatives.

As an extension of our previous studies on the reactivity of 8-trifluoromethanesulfonyl- and 8-aryl-CHFs, we explored the incorporation of aryl groups at both the 3- and 8-positions of these molecules. The introduction of two aryl groups into CHF can effectively achieve a redshift of its absorption wavelength due to the extension of the conjugated system, leading to the development of its application in functional dyes. *p*-Methoxy and *p*-nitrophenyl groups were selected and introduced as the aryl groups to be introduced. The incorporation of these aryl groups with different electronic properties is anticipated to induce donor-acceptor-type contributions, thereby endowing the modified molecules with optical properties that are significantly different from those exhibited by conventional CHFs.

In this paper, we describe the synthesis and properties of 3,8-diaryl-CHFs, which were prepared via the Suzuki-Miyaura coupling reaction. The optical and structural properties of 3,8-diaryl-CHFs were investigated by UV/Vis spectroscopy, theoretical calculations, and single-crystal X-ray analysis. In addition, the redox behavior of these compounds was investigated by voltammetry experiments, i.e., cyclic voltammetry (CV) and differential pulse voltammetry (DPV). The results indicate that the aryl groups at the 3- and 8-positions significantly affect the electronic properties of the CHFs, leading to unique optical and electrochemical properties contingent on the electronic nature of the aryl groups substituted.

2. Results and Discussion

Synthesis: The preparation of **4a**–**4c** began with the treatment of **1** or **2a**–**2c** [11] using *N*-iodosuccinimide (NIS), followed by the Suzuki–Miyaura coupling [28] with phenylboronic acid (Figure 2). Owing to the instability and rapid decomposition of the iodide intermediate **3** during the purification process, we performed the subsequent Suzuki–Miyaura coupling without the isolation of **3** using $PdCl_2$(dppf) as a catalyst. As a result, the coupling product **4a** at the 3- and 8-positions was obtained in a 50% yield in a one-pot procedure. The reaction of **2a** with NIS also provided an unstable product; hence, the coupling reaction with phenylboronic acid was performed without a purification process to give **4a** in a 60% yield. In a similar manner, iodation of **2b** and **2c** with NIS and the following Suzuki–Miyaura coupling with *p*-nitrophenylboronic or *p*-methoxyphenylboronic acids formed the corresponding coupling products **4b** and **4c** in 77% and 40% yields, respectively, in the two steps. The resulting **4a**–**4c** demonstrated sufficient stability to be stored for several months under ambient conditions.

Spectroscopic properties: Newly prepared compounds **4a**–**4c** were comprehensively characterized utilizing spectral data, as detailed in the "Materials and Methods" section. Charts of NMR and high-resolution mass spectra (HRMS) of **4a**–**4c** were appeared in Supplementary Materials. The ^{1}H NMR spectroscopic assignments of **4a**–**4c** were validated by the COSY experiment. The HRMS of **4a**–**4c**, ionized through electrospray ionization (ESI), exhibited the expected molecular ion peaks, corroborating their molecular structures.

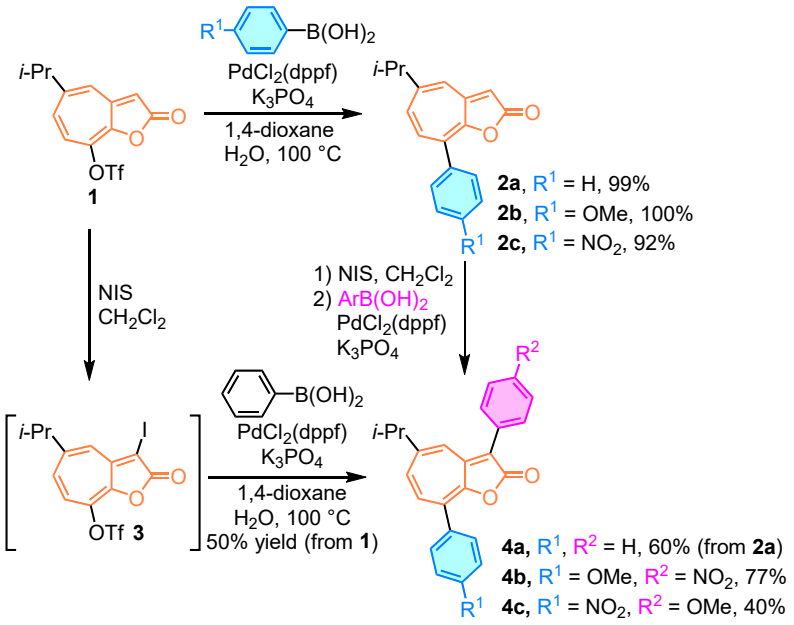

Figure 2. Synthesis of 3,8-diaryl-CHFs **4a**–**4c**.

Due to the acquisition of suitable crystals by slow solvent evaporation, the molecular structures of **4a**–**4c** were elucidated by X-ray crystallographic analysis, as depicted in Figure 3. Previously, we reported that the CHF moiety and substituted aryl groups of 8-aryl-CHFs have large dihedral angles and that the contribution of these conjugates is small based on their UV/Vis spectra. On the other hand, the dihedral angles between the CHF moiety and phenyl groups at the 3-position and at the 8-position of **4a** were 39.58° and 34.78°, respectively, which are smaller than those of the 8-aryl-CHFs. Although the dihedral angle (40.26°) between the CHF moiety and the aryl group at the 3-position of **4b** was similar to that of **4a**, the angle with the aryl group at the 8-position (58.10°) was comparable to those in 8-aryl-CHFs. Similar to **4b**, a larger dihedral angle (65.71°) between the CHF moiety and the aryl group at the 8-position was observed in **4c**,even though that at the 3-position is relatively small (35.63°). This observation implies that the aryl group at the 3-position of **4b** and **4c** may extend the conjugated system, whereas the aryl group at the 8-position may not significantly contribute to the π-extension.

To evaluate the optical properties of the prepared compounds, measurements of their UV/Vis absorption spectra were performed. The absorption maxima and coefficients (log ε) of **4a**–**4c** in CH_2Cl_2 and **2a**–**2c** as a reference are shown in Table 1. The UV/Vis spectra of **4a**–**4c** are represented in Figure 4.

Table 1. The longest absorption maxima [nm] and their coefficients (log ε) of **4a**–**4c** in CH_2Cl_2 and **2a**–**2c** in CH_2Cl_2 as a reference, and electronic transitions of **4a**–**4c** derived from the computed values based on the TD-DFT calculations at the B3LYP/6-31+G* level.

	Experimental	Computed Values	
Compound	**λ_{max} [nm] (log ε)**	**λ_{max} (Oscillator Strength)**	**Composition of Band (Contribution)**
4a	411 (4.26)	454 (0.0168)	H → L (0.6044) H → L + 1 (0.3550) H − 1 → L (0.0863)
		366 (0.5569)	H → L (0.2631) H → L + 1 (0.5405)

Table 1. *Cont.*

Compound	Experimental	Computed Values	
	λ_{max} [nm] (log ε)	λ_{max} (Oscillator Strength)	Composition of Band (Contribution)
4b	443 (4.42)	446 (0.0517)	H → L (0.2436) H → L + 1 (0.6598) H → L + 2 (0.0471)
		421 (0.7559)	H → L (0.6154) H → L + 1 (0.2990)
4c	424 (4.25)	519 (0.1046)	H → L (0.7916) H → L + 1 (0.1354) H → L + 2 (0.0458)
		458 (0.1429)	H → L (0.1216) H → L + 1 (0.8431)
		379 (0.3522)	H − 1 → L (0.1842) H → L + 2 (0.7128)
2a	395 (4.06)	–	–
2b	396 (4.09)	–	–
2c	396 (4.10)	–	–

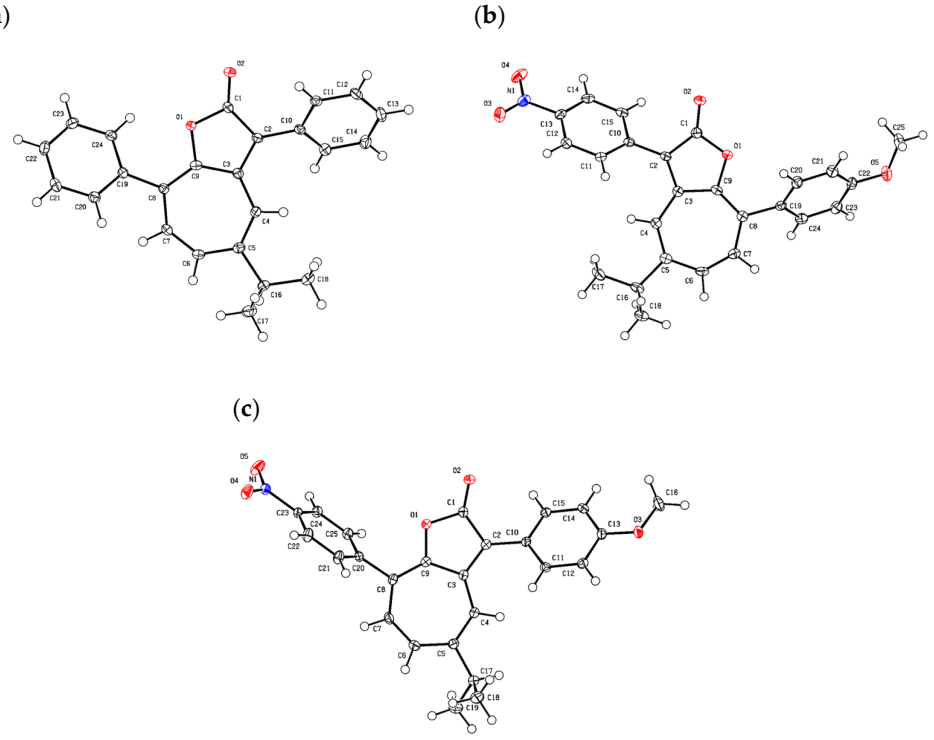

Figure 3. ORTEP drawing of (**a**) **4a** (CCDC2145584), (**b**) **4b** (CCDC2290744), and (**c**) **4c** (CCDC2361752) [29].

The maximum absorption wavelengths of **4a**–**4c** displayed a redshift from those of the corresponding **2a**–**2c**. For instance, the absorption maxima of **4a** (λ_{max} = 411 nm) exhibit a redshift of 16 nm compared to that of **2a** (λ_{max} = 395 nm), suggesting that the aryl group introduced at the 3-position effectively extends the conjugated system as predicted by the single-crystal X-ray analysis. Compounds **4b** (λ_{max} = 443 nm) and **4c** (λ_{max} = 424 nm), which incorporate both an electron-donating *p*-methoxyphenyl and an electron-withdrawing *p*-nitrophenyl group within their structures, exhibit absorption at the longer wavelength region, compared to that of **4a**. However, the maximum absorption wavelength of **4b** displayed a redshift of 19 nm compared to that of **4c**. These results suggest that the

introduction of an electron-withdrawing group (EWG), i.e., the *p*-nitrophenyl group, at the 3-position of CHF leads to a longer wavelength of maximum absorption than at the 8-position.

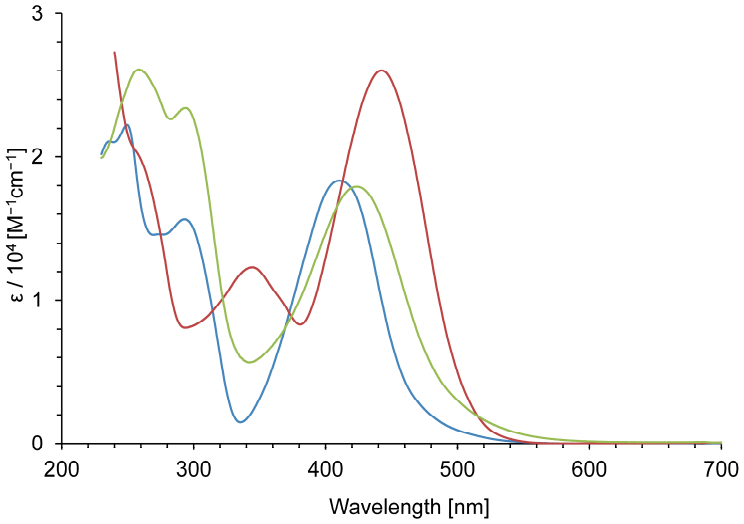

Figure 4. UV/Vis spectra of **4a** (blue line), **4b** (red line), and **4c** (light-green line) in CH_2Cl_2.

To theoretically elucidate the variations in absorption wavelengths observed in the UV/Vis spectra of **4a**–**4c**, the electronic transitions within the absorption band and the energies of the HOMO and LUMO of these compounds were examined using time-dependent density functional theory (TD-DFT) calculations at the B3LYP/6-31G* level [30]. These methods are employed to optimize the molecular geometries, calculate the electronic excitation energies, and determine the UV/Vis absorption spectra. The electronic transitions of **4a**–**4c**, as determined from the calculations, are summarized in Table 1. Figure 5 represents the frontier Kohn–Sham orbitals of **4a**–**4c** along with their corresponding energy levels.

Theoretical calculations indicated that the absorption bands in the visible region for **4a**–**4c** result from the superposition of multiple transitions. The longest wavelength absorption band of **4a** was revealed as the transitions between HOMO, HOMO−1, and LUMO, LUMO+1, and in these, there is hardly any orbital coefficient involved in the LUMOs of the phenyl groups at the 3- and 8-positions. Therefore, this absorption band in **4a** is considered to be dominated by the π-π* transition of CHF itself. The absorption band of **4b** was also revealed as transitions from HOMO, in which the orbital coefficients are distributed in the aryl groups at the 3- and 8-positions and in the CHF moiety, to LUMO, LUMO+1, and LUMO+2. Among these transitions, the HOMO–LUMO transition, specifically the π-π* transition and the intramolecular charge transfer between the two aryl groups, was identified as the dominant contribution based on the calculation results. The longest absorption band of **4c** can be attributed to the overlap of several transitions from HOMO, HOMO−1 to LUMO, LUMO+1, and LUMO+2. The maximum absorption wavelength of **4c** shows a hypochromic shift compared to that of **4b**, but the absorption onset wavelength was observed to be on the longer side, which could be attributed to the HOMO to LUMOs transitions, i.e., both of π-π* transitions, and the intramolecular charge transfer between the *p*-methoxyphenyl and *p*-nitrophenyl groups at the 3- and 8-positions, i.e., transition from HOMO to LUMO and LUMO+2.

To elucidate the electrochemical properties, the redox potentials of **4a**–**4c** were assessed by CV and DPV. The redox potentials derived from DPV measurements are summarized in Table 2.

Table 2. Redox potentials measured by DPV [a] of **4a**–**4c**.

Compound	E_1^{OX} [V]	E_2^{OX} [V]	E_3^{OX} [V]	E_1^{RED} [V]	E_2^{RED} [V]	E_3^{RED} [V]
4a	+0.91	–	–	−1.72	–	–
4b	+1.02	+1.30	+1.43	−1.38	−1.71	−1.88
4c	+0.84	+1.50	–	−1.34	−1.48	−1.86

V vs. $Ag/AgNO_3$, 1 mM in benzonitrile containing Et_4NClO_4 (0.1 M), Pt electrode (internal diameter: 1.6 mm), scan rate: 20 mVs^{-1}, and internal reference Fc/Fc^+ = +0.15 V.

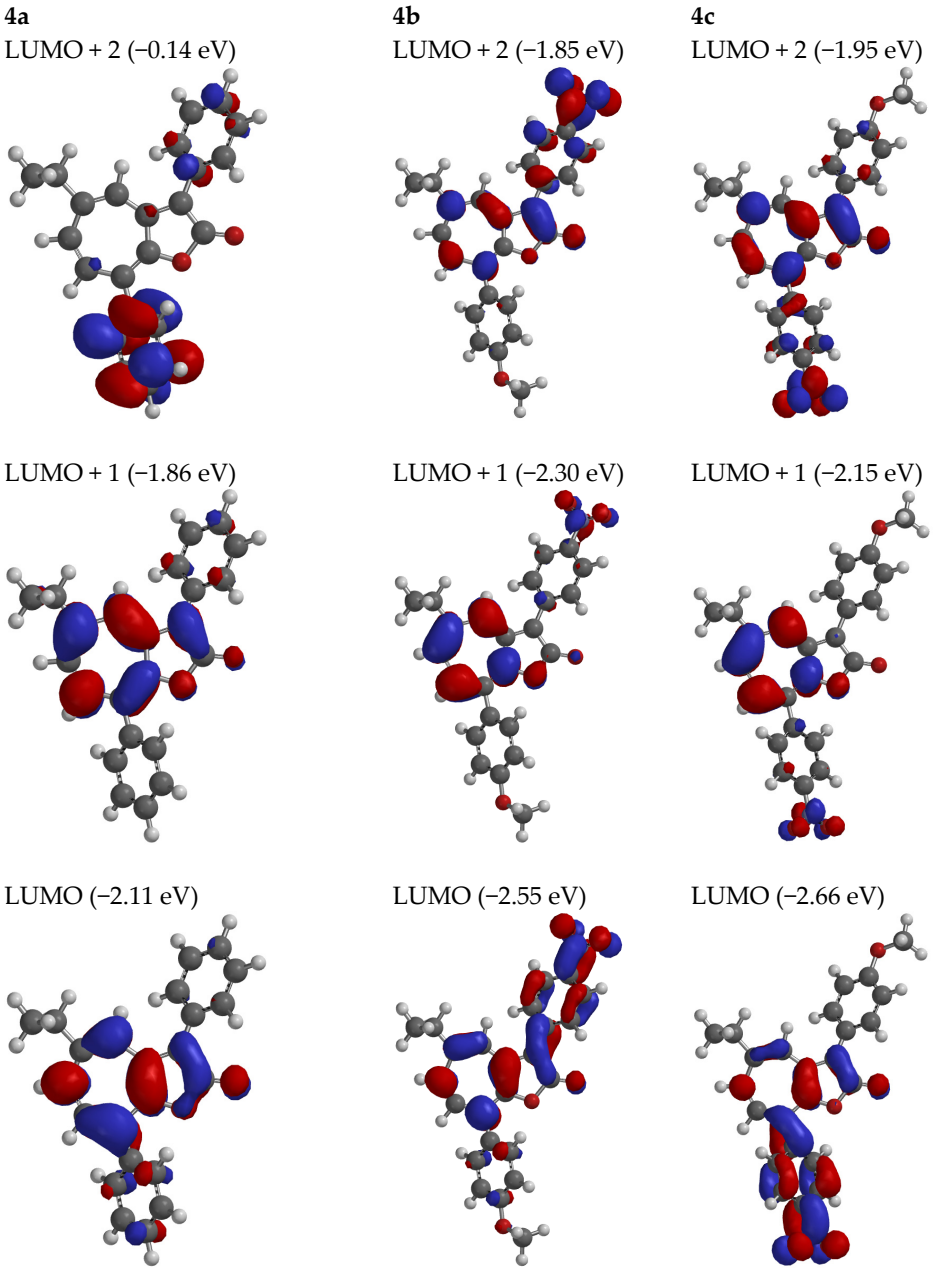

Figure 5. *Cont.*

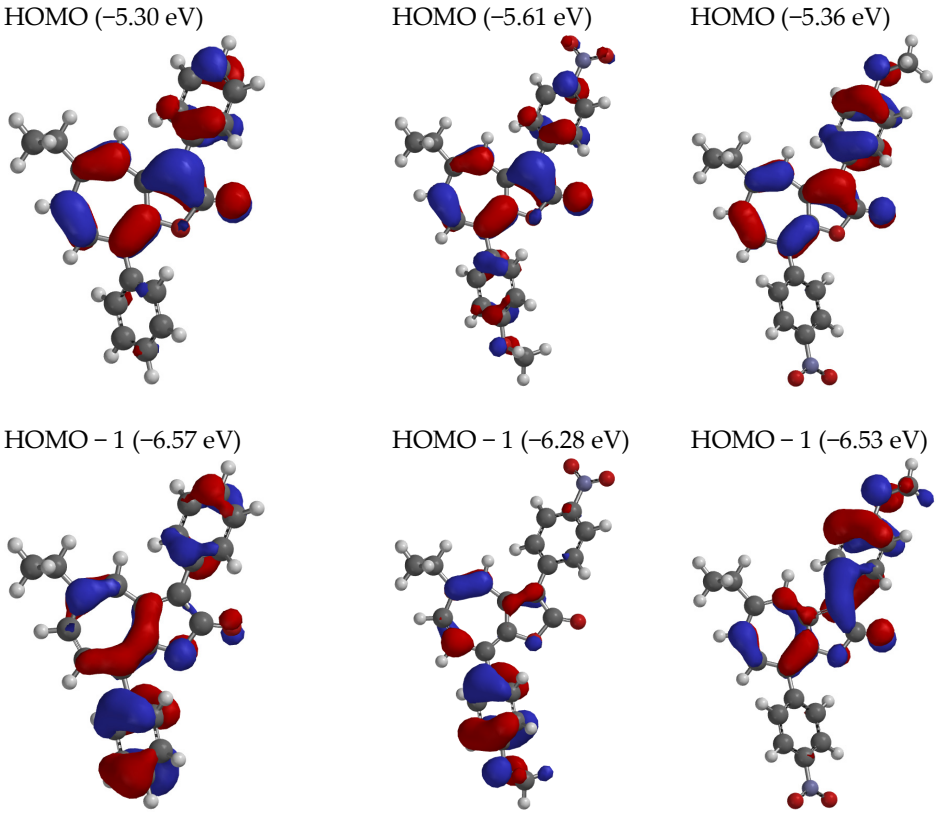

Figure 5. Frontier Kohn–Sham orbitals and their energy levels of **4a** (left), **4b** (center), and **4c** (right) at the B3LYP/6-31G* level.

Cyclic voltammograms of **4a**–**4c** displayed irreversible redox waves under CV measurement conditions, suggesting the formation of unstable cationic and anionic species. The first oxidation potential (E_1^{OX}) in the DPV of **4b** (+1.02 V) showed an anodic shift compared to that of **4a** (+0.91 V). On the other hand, a cathodic shift was observed in the E_1^{OX} of **4c** (+0.84 V) relative to **4a**. These results imply the EWG at the 3-position of **4b**, i.e., the *p*-nitrophenyl group, is accountable for the reduction in the energy level of HOMO, as anticipated by DFT calculations. The first reduction potential (E_1^{RED}) of **4a** displayed −1.72 V, while those of **4b** (−1.38 V) and **4c** (−1.34 V) were almost the same. These identical E_1^{RED} values were attributed to the reduction in the substituted *p*-nitrophenyl group of **4b** and **4c**, rather than CHF moiety, under the electrochemical reduction conditions. These results indicate that the LUMO energy level, unlike that of HOMO, is decreased by the EWG at the 3- or 8-positions, as expected from the DFT calculations. Since the value of E_2^{RED} in **4b** (−1.71 V) is similar to E_1^{RED} of **4a**, this peak potential can be corresponded to the electrochemical reduction in the CHF moiety. Meanwhile, the E_2^{RED} of **4c** (−1.48 V) revealed a pronounced cathodic shift compared to that of **4b**. This outcome implies that the substitution of a *p*-nitrophenyl group at the 8-position effectively reduces the reduction potential of the CHF moiety more than the substitution at the 3-position.

3. Materials and Methods

Melting points were determined with a Yanagimoto MPS3 micro-melting apparatus and are uncorrected. High-resolution mass spectra were obtained with a Waters Xevo G2-XS QTof instrument. The UV/Vis spectra were recorded with a Shimadzu UV-2550 spectrophotometer (Shimadzu Corporation, Kyoto, Japan). Voltammetry measurements were carried out with a BAS 100B/W electrochemical workstation (BAS Corporation, Tokyo, Japan). ^{1}H and ^{13}C NMR spectra were recorded in $CDCl_3$ with a JEOL ECA500 at 500 MHz and 125 MHz or a JEOL ECZ400 at 400 MHz and 100 MHz (JEOL Ltd., Tokyo, Japan), respectively.

5-Isopropyl-3,8-diphenyl-2*H*-cyclohepta[*b*]furan-2-one (**4a**): Synthesis from **1**: To a solution of **1** (168 mg, 0.50 mmol) in CH_2Cl_2 (2.5 mL) was added *N*-iodosuccinimide (169 mg, 0.75 mmol) at room temperature. The resulting mixture was stirred at the same temperature for 1 h. After the solvent was removed under reduced pressure, the crude product was passed through the short silica gel column with $CHCl_3$ to give crude iodide **3** (113 mg). To a degassed solution of the crude iodide **3**, phenylboronic acid (92 mg, 0.754 mmol), K_3PO_4 (317 mg, 1.49 mmol) in 1,4-dioxane (1.2 mL) and H_2O (0.2 mL) were added $PdCl_2$(dppf) (11 mg, 0.01 mmol). The resulting mixture was stirred at 100 °C for 13 h. The reaction mixture was poured into water and extracted with AcOEt. The organic layer was washed with brine, dried over Na_2SO_4, and concentrated under reduced pressure. The residue was purified by column chromatography on silica gel with $CHCl_3$/AcOEt (50:1) as an eluent to give **4a** (85 mg, 50% from **1**) as yellow solid.

Synthesis from **2a**: To a solution of **2a** (267 mg, 1.01 mmol) in CH_2Cl_2 (5 mL) was added *N*-iodosuccinimide (338 mg, 1.50 mmol) at room temperature. The resulting mixture was stirred at the same temperature for 1 h. After the solvent was removed under reduced pressure, the crude product was passed through the silica gel column with $CHCl_3$/AcOEt (20:1) to give crude iodide (383 mg). To a degassed solution of the crude iodide, phenylboronic acid (177 mg, 1.45 mmol), K_3PO_4 (616 mg, 2.90 mmol) in 1,4-dioxane (5 mL) and H_2O (0.5 mL) were added $PdCl_2$(dppf) (37 mg, 0.05 mmol). The resulting mixture was stirred at 100 °C for 13 h. The reaction mixture was poured into water and extracted with AcOEt. The organic layer was washed with brine, dried over Na_2SO_4, and concentrated under reduced pressure. The residue was purified by column chromatography on silica gel with $CHCl_3$/AcOEt (50:1) as an eluent to give **4a** (206 mg, 60% from **2a**) as yellow solid. M.p. 190–191 °C; UV/Vis (CH_2Cl_2): λ_{max} (log ε) = 236 (4.32), 250 (4.35), 293 (4.19), 410 (4.26) nm; ^{1}H NMR (500 MHz, $CDCl_3$): δ_H = 7.64 (dd, *J* = 8.0, 1.1 Hz, 2H, Ph), 7.55–7.54 (m, 3H, H_4, Ph), 7.45–7.51 (m, 4H, Ph), 7.36–7.43 (m, 2H, Ph), 7.08 (d, *J* = 12.1 Hz, 1H, H_7), 6.77 (dd, *J* = 12.1, 1.6 Hz, 1H, H_6), 2.80 (sept, *J* = 6.9 Hz, 1H, *i*-Pr), 1.25 (d, *J* = 6.9 Hz, 6H, *i*-Pr) ppm; ^{13}C NMR (125 MHz, $CDCl_3$): δ_C = 168.45, 154.99, 152.97, 146.53, 137.66, 136.33, 131.41, 130.96, 129.45, 128.85, 128.59, 128.53, 127.90, 127.32, 123.54, 110.05, 38.66, 23.05 ppm; HRMS (ESI-TOF): calcd for $C_{24}H_{20}O_2$ + Na^+ $[M + Na]^+$ 363.1355, found: 363.1375.

5-Isopropyl-3-(4-nitrophenyl)-8-(4-methoxyphenyl)-2*H*-cyclohepta[*b*]furan-2-one (**4b**): To a solution of **2b** (301 mg, 1.02 mmol) in CH_2Cl_2 (5 mL) was added *N*-iodosuccinimide (345 mg, 1.54 mmol) at room temperature. The resulting mixture was stirred at the same temperature for 1 h. After the solvent was removed under reduced pressure, the crude product was passed through the silica gel column with $CHCl_3$/AcOEt (20:1) to give crude iodide (397 mg). To a degassed solution of the crude iodide, *p*-methoxyphenylboronic acid (237 mg, 1.42 mmol), K_3PO_4 (605 mg, 2.85 mmol) in 1,4-dioxane (5 mL) and H_2O (0.5 mL) were added $PdCl_2$(dppf) (39 mg, 0.05 mmol). The resulting mixture was stirred at 100 °C for 12.5 h. The reaction mixture was poured into water and extracted with AcOEt. The organic layer was washed with brine, dried over Na_2SO_4, and concentrated under reduced pressure. The residue was purified by column chromatography on silica gel with $CHCl_3$/AcOEt (20:1) as an eluent to give **4b** (328 mg, 77% from **2b**) as orange solid. M.p. 227–229 °C; UV/Vis (CH_2Cl_2): λ_{max} (log ε) = 344 (4.09), 443 (4.42) nm; ^{1}H NMR (500 MHz, $CDCl_3$): δ_H = 8.32 (d, *J* = 8.9 Hz, 2H, 3-(*m*-Bz)), 7.84 (d, *J* = 8.9 Hz, 2H, 3-(*o*-Bz)), 7.61 (s, 1H, H_4), 7.53 (d, *J* = 8.9 Hz, 2H, 8-(*m*-Bz)), 7.25 (d, *J* = 12.2 Hz, 1H, H_7), 7.00 (d, *J* = 8.9 Hz, 2H, 8-(*o*-Bz)), 6.92 (dd, *J* = 12.2, 1.6 Hz, 1H, H_6), 3.87 (s, 3H, OMe), 2.88 (sept, *J* = 6.9 Hz, 1H, *i*-Pr), 1.28 (d, *J* = 6.9 Hz, 6H, *i*-Pr) ppm; ^{13}C NMR (125 MHz, $CDCl_3$): δ_C = 167.63, 160.21, 156.89, 152.89, 147.47, 146.53, 138.48, 137.56, 132.33, 131.01, 129.47, 129.21, 128.97, 124.10, 123.26, 114.15, 106.53, 77.36, 55.49, 38.83, 23.16 ppm; HRMS (ESI-TOF): calcd for $C_{25}H_{21}NO_5$ + H^+ $[M + H]^+$ 416.1493, found: 416.1479.

5-Isopropyl-3-(4-methoxyphenyl)-8-(4-nitrophenyl)-2*H*-cyclohepta[*b*]furan-2-one (**4c**): To a solution of **2c** (235 mg, 0.76 mmol) in CH_2Cl_2 (5 mL) *N*-iodosuccinimide (280 mg, 1.24 mmol) was added at room temperature. The resulting mixture was stirred at the same temperature for 1 h. After the solvent was removed under reduced pressure, the crude

product was passed through the silica gel column with $CHCl_3$/AcOEt (50:1) to give crude iodide (312 mg). To a degassed solution of the crude iodide, *p*-nitrophenylboronic acid (167 mg, 1.01 mmol), K_3PO_4 (471 mg, 2.22 mmol) in 1,4-dioxane (5 mL) and H_2O (0.5 mL) were added $PdCl_2$(dppf) (37 mg, 0.04 mmol). The resulting mixture was stirred at 100 °C for 15 h. The reaction mixture was poured into water and extracted with AcOEt. The organic layer was washed with brine, dried over Na_2SO_4, and concentrated under reduced pressure. The residue was purified by column chromatography on silica gel with $CHCl_3$ as an eluent to give **4c** (127 mg, 40% from **2c**) as red solid. M.p. 234–235 °C; UV/Vis (CH_2Cl_2): λ_{max} (log ε) = 258 (4.42), 293 (4.37), 424 (4.25) nm; ^{1}H NMR (400 MHz, $CDCl_3$): δ_H = 8.30 (d, *J* = 8.7 Hz, 2H, 8-(*m*-Bz)), 7.70 (d, *J* = 8.7 Hz, 2H, 8-(*o*-Bz)), 7.55 (d, *J* = 8.7 Hz, 2H, 3-(*o*-Bz)), 7.48 (d, *J* = 1.4 Hz, 1H, H_4), 7.02 (d, *J* = 9.1 Hz, 2H, 3-(*m*-Bz)), 6.92 (d, *J* = 12.3 Hz, 1H, H_7), 6.74 (dd, *J* = 12.3, 1.4 Hz, 1H, H_6), 3.86 (s, 3H, OMe), 2.79 (sept, *J* = 6.9 Hz, 1H, *i*-Pr), 1.25 (d, *J* = 6.9 Hz, 6H, *i*-Pr) ppm; ^{13}C NMR (100 MHz, $CDCl_3$): δ_C = 168.07, 159.51, 154.81, 153.26, 147.47, 145.40, 144.14, 134.34, 131.82, 130.47, 129.79, 123.83, 123.68, 122.62, 114.37, 111.09, 55.40, 38.63, 22.92 ppm; HRMS (ESI-TOF): calcd for $C_{25}H_{21}NO_5$ + H^+ $[M + H]^+$ 416.1493, found: 416.1519.

4. Conclusions

In this study, we have successfully prepared and characterized a series of 3,8-diaryl-2*H*-cyclohepta[*b*]furan-2-ones **4a**–**4c** using a one-pot procedure involving sequential iodation and Suzuki–Miyaura coupling.

The introduction of aryl groups at both the 3- and 8-positions of CHFs has been shown to influence their electronic properties, resulting in distinct optical and electrochemical behaviors. The optical properties of **4a**–**4c**, evaluated through UV/Vis spectroscopy, indicated that the substitution of aryl groups extends the conjugated system, leading to a bathochromic shift in the absorption maxima. In particular, the introduction of a p-nitrophenyl group at the 3-position of CHF led to a redshift of the maximum absorption wavelength. This was corroborated by theoretical calculations, which revealed that the absorption bands of these compounds are primarily due to π-π* transitions and intramolecular charge transfer between the aryl groups.

Electrochemical analysis of **4a**–**4c** via CV and DPV demonstrated that these compounds exhibit irreversible redox waves, indicative of the formation of unstable cationic and anionic species under the redox conditions. The redox potentials of **4a**–**4c** were also found to be influenced by the nature of the aryl substituents, with electron-donating and EWG affecting the HOMO and LUMO energy levels as predicted by DFT calculations.

As mentioned in the introduction, 2*H*-cyclohepta[*b*]furan-2-ones are useful precursors of azulene derivatives. Thus, **4a**–**4c** could also be convertible to novel azulene derivatives. Therefore, we currently investigate the efficient synthesis of azulene derivatives using **4a**–**4c** as starting materials.

Supplementary Materials: The following supporting information can be downloaded at: https://www.mdpi.com/article/10.3390/org5030013/s1, Supplementary File S1: charts of ^{1}H NMR, ^{13}C NMR, COSY, and HRMS spectra, UV/Vis spectra, cyclic voltammograms, and ORTEP drawing of **4a**–**4c**.

Author Contributions: Conceptualization, T.S.; methodology, T.S. and D.A.; formal analysis, T.S., D.A., M.I., T.O., R.S. and S.I.; investigation, T.S., D.A., M.I., T.O., R.S. and S.I.; resources, T.S., D.A., M.I., T.O., R.S. and S.I.; writing—original draft preparation, T.S.; writing—review and editing, T.S., D.A., M.I., T.O., R.S. and S.I.; supervision, T.S.; funding acquisition, T.S. All authors have read and agreed to the published version of the manuscript.

Funding: This work was supported by JSPS KAKENHI Grant Number 21K05037.

Data Availability Statement: The data of this study are available in the Supporting Information of this article, or via request from the corresponding author.

Conflicts of Interest: The authors declare no conflicts of interest.

References

1. Morita, N.; Toyota, K.; Ito, S. The Chemistry of 2*H*-Cyclohepta[*b*]Furan-2-One: Synthesis, Transformation and Spectral Properties. *Heterocycles* **2009**, *78*, 1917–1954. [CrossRef]
2. Yokota, M.; Yanagisawa, T.; Kosakai, K.; Wakabayashi, S.; Tomiyama, T.; Yasunami, M. Synthesis and Analysis of Positive Inotropic Effects of 3-Substituted-2*H*-Cyclohepta[*b*]Furan-2-One Derivatives. *Chem. Pharm. Bull.* **1994**, *42*, 865–871. [CrossRef]
3. Ando, M.; Kataoka, N.; Yasunami, M.; Takase, K.; Hirata, N.; Yanagi, Y. Tropolone Derivatives as Synthetic Intermediates. 1. A Novel Synthetic Method of the Octahydro-2H-Cyclohepta[*b*]Furan-2-One Derivatives. *J. Org. Chem.* **1987**, *52*, 1429–1437. [CrossRef]
4. Shimoma, F.; Kusaka, H.; Wada, K.; Azami, H.; Yasunami, M.; Suzuki, T.; Hagiwara, H.; Ando, M. A Novel Synthetic Method of the (±)-(3aα,8aα)-Ethyl 8β-Hydroxy-6β-Methyl-2-Oxooctahydro-2H-Cyclohepta[*b*]Furan-3α- Carboxylate and Its Chemical Transformation to (±)-(3aα,8aα)-3α,6β-Dimethyl-3,3a,4,5,6,8a-Hexahydro-2H- Cyclohepta[*b*]Furan-2-One, (+)- and (−)-7β-(2-Acetoxy-1α-Methylethyl)-4β-Methyl-2-Cyclohepten-1β-Ol, and (+)- and (−)-7β-(2-Acetoxy-1α-Methylethyl)-4β-Methyl-2-Cyclohepten-1-One. Possible Common Synthetic Intermediates for Pseudoguaianolides, 4,5-Secopseudoguaianolides, Guaianolides, 4,5-Secoguaianolides, and Octalactins. *J. Org. Chem.* **1998**, *63*, 920–929.
5. Shimoma, F.; Kusaka, H.; Azami, H.; Wada, K.; Suzuki, T.; Hagiwara, H.; Ando, M. Total Syntheses of (±)-Hymenolin and (±)-Parthenin. *J. Org. Chem.* **1998**, *63*, 3758–3763. [CrossRef]
6. Naya, S.; Nitta, M. Synthesis and Properties of Stable Heteroazulene Analogues of a Triphenylmethyl Cation. *J. Chem. Soc. Perkin Trans.* **2000**, *1*, 2777–2781. [CrossRef]
7. Naya, S.; Nitta, M. Synthesis and Properties of Stabilized Bis(2-Oxo-2H-Cyclohepta[*b*]Furan-3-Yl)Phenylmethyl and Bis(1,2-Dihydro-2-Oxo-N-Phenylcyclohepta[*b*]Pyrrol-3-Yl)Phenylmethyl Cations and Their Derivatives: Remarkable Substituent Effect on the Conformation and Stability of the Cations. *J. Chem. Soc. Perkin Trans.* **2000**, *2*, 2427–2435.
8. Naya, S.; Nitta, M. Dication Species Stabilized by Heteroazulenes: Synthesis and Properties of 1,3- and 1,4-Bis[Bis(2-Oxo-2H-Cyclohepta[*b*]Furan-3-Yl)Methyliumyl]-, Bis[Bis(1,2-Dihydro-N-Methyl-2-Oxocyclohepta[*b*]Pyrrol-3-Yl)Methyliumyl]Benzene, and Their Related Dications. *J. Chem. Soc. Perkin Trans.* **2001**, *2*, 275–281. [CrossRef]
9. Naya, S.; Sakakibara, T.; Nitta, M. Stability of Heteroazulene-Substituted Tropylium Ions: Synthesis and Properties of the (2-Oxo-2H-Cyclohepta[*b*]Thiophen-3-Yl)Tropylium Ion, and Its Oxygen and Nitrogen Analogues. *J. Chem. Soc. Perkin Trans.* **2001**, *2*, 1032–1037. [CrossRef]
10. Naya, S.; Isobe, M.; Hano, Y.; Nitta, M. Trication Species Stabilized by Heteroazulenes: Synthesis and Properties of 1,3,5-Tris[Bis(Heteroazulen-3-Yl)Methyliumyl]Benzenes. *J. Chem. Soc. Perkin Trans.* **2001**, *2*, 2253–2262. [CrossRef]
11. Nozoe, T.; Yang, P.-W.; Wu, C.-P.; Huang, T.-S.; Lee, T.-H.; Okai, H.; Wakabayashi, H.; Ishikawa, S. A Convenient, One-pot Azulene Synthesis from Cyclohepta[*b*]furan-2-ones and Vinyl Ether and Its Analogues (I). Vinyl Ethyl Ether, Vinyl Acetates, Dihydrofurans, and Dihydropyrans as Reagent. *Heterocycles* **1989**, *29*, 1225–1232.
12. Nozoe, T.; Wakabayashi, H.; Shindo, K.; Ishikawa, S.; Wu, C.-P.; Yang, P.-W. A Convenient, One-Pot Azulene Synthesis from 2*H*-cyclohepta[*b*]furan-2-ones with Vinyl Ether and Its Analogues III. Orthoesters as a reagent. *Heterocycles* **1991**, *32*, 213–220.
13. Wakabayashi, H.; Yang, P.-W.; Wu, C.-P.; Shindo, K.; Ishikawa, S.; Nozoe, T. A Convenient, One-Pot Synthesis of Azulenes Having Versatile Functional Groups by the Reaction of 2*H*-cyclohepta[*b*]furan-2-ones with Furan Derivatives. *Heterocycles* **1992**, *34*, 429–434. [CrossRef]
14. Yasunami, M.; Kitamori, Y.; Kikuchi, I.; Ohmi, H.; Takase, K. Peri-Selective Cycloaddition Reactions of 3-Methoxycarbonyl-2*H*cyclohepta[*b*]furan-2-one with 6,6-Dimethylfulvene. *Bull. Chem. Soc. Jpn.* **1992**, *65*, 2127–2130. [CrossRef]
15. Yasunami, M.; Takase, K. The Syntheses of Azulene Derivatives by the Reaction of 2*H*-cyclohepta[*b*]furan-2-ones with Enamines. *J. Syn. Org. Chem. Jpn.* **1981**, *39*, 1172–1182.
16. Yang, P.-W.; Yasunami, M.; Takase, K. The formation of azulene derivatives by the reaction of 2*H*-cyclohepta[*b*]furan-2-ones with enamines. *Tetrahedron Lett.* **1971**, *12*, 4275–4278. [CrossRef]
17. Yasunami, M.; Chen, A.; Yang, P.-W.; Takase, K. The Facile Synthesis of 1- and 2-Alkylazulenes by the Reactions of 2*H*cyclohepta[*b*]furan-2-ones with Enamines of Aldehydes and Acyclic Ketones. *Chem. Lett.* **1980**, *9*, 579–582. [CrossRef]
18. Yasunami, M.; Miyoshi, S.; Kanegae, N.; Takase, K. A Versatile Synthetic Method of 1-Alkylazulenes and Azulene by the Reactions of 3-Methoxycarbonyl-2*H*-cyclohepta[*b*]furan-2-one with in situ Generated Enamines. *Bull. Chem. Soc. Jpn.* **1993**, *66*, 892–899. [CrossRef]
19. Shoji, T.; Sugiyama, S.; Kobayashi, Y.; Yamazaki, A.; Ariga, Y.; Katoh, R.; Wakui, H.; Yasunami, M.; Ito, S. Direct synthesis of 2-arylazulenes by [8 + 2] cycloaddition of 2*H*-cyclohepta[*b*]furan-2-ones with silyl enol ethers. *Chem. Commun.* **2020**, *56*, 1485–1488. [CrossRef] [PubMed]
20. Shoji, T.; Ito, S.; Yasunami, M. Synthesis of Azulene Derivatives from 2*H*-Cyclohepta[*b*]Furan-2-Ones as Starting Materials: Their Reactivity and Properties. *Int. J. Mol. Sci.* **2021**, *22*, 10686. [CrossRef] [PubMed]
21. Morita, N.; Matsuki, T.; Nakashima, M.; Shoji, T.; Toyota, K.; Kikuchi, S.; Ito, S. Reaction of 2*H*-Cyclohepta[*b*]Furan-2-Ones with Pyridinium Salts of Trifluoromethanesulfonic Anhydride. *Heterocycles* **2006**, *69*, 119–122. [CrossRef]
22. Morita, N.; Higashi, J.; Okada, K.; Shoji, T.; Toyota, K.; Watanabe, M.; Yasunami, M.; Kikuchi, S.; Ito, S. Synthesis and Reactivity of 3-Methylsulfinyl-2*H*-Cyclohepta[*b*]Furan-2-Ones. *Heterocycles* **2008**, *76*, 759–770. [CrossRef]
23. Shoji, T.; Higashi, J.; Ito, S.; Oda, M.; Yasunami, M.; Morita, N. Synthesis and Redox Behavior of Cyanovinyl-Substituted 2*H*-Cyclohepta[*b*]Furan-2-Ones. *Heterocycles* **2012**, *86*, 305–315. [CrossRef]

24. Shoji, T.; Higashi, J.; Ito, S.; Okujima, T.; Yasunami, M.; Morita, N. Synthesis of Redox-Active, Intramolecular Charge-Transfer Chromophores by the [2+2] Cycloaddition of Ethynylated 2*H*-Cyclohepta[*b*]Furan-2-ones with Tetracyanoethylene. *Chem. Eur. J.* **2011**, *17*, 5116–5129. [CrossRef]
25. Shoji, T.; Higashi, J.; Ito, S.; Okujima, T.; Yasunami, M.; Morita, N. Synthesis of Donor–Acceptor Chromophores by the [2+2] Cycloaddition of Arylethynyl-2*H*-Cyclohepta[*b*]Furan-2-Ones with 7,7,8,8-Tetracyanoquinodimethane. *Org. Biomol. Chem.* **2012**, *10*, 2431–2438. [CrossRef]
26. Shoji, T.; Morita, N.; Maruyama, M.; Shimomura, E.; Maruyama, A.; Ito, S.; Yasunami, M.; Higashi, J.; Toyota, K. Synthesis, Properties, and Crystal Structure of DDQ-Adducts of Ethynylated 2*H*-Cyclohepta[*b*]Furan-2-Ones. *Heterocycles* **2014**, *88*, 319–329. [CrossRef]
27. Shoji, T.; Ando, D.; Yamazaki, A.; Ariga, Y.; Hamasaki, A.; Mori, S.; Okujima, T.; Ito, S. Synthesis of 8-Aryl-2*H*-Cyclohepta[*b*]Furan-2-Ones and Transformation into 4-Arylazulenes. *Chem. Lett.* **2022**, *51*, 533–537. [CrossRef]
28. Miyaura, N.; Suzuki, A. Palladium-Catalyzed Cross-Coupling Reactions of Organoboron Compounds. *Chem. Rev.* **1995**, *95*, 2457–2483. [CrossRef]
29. CCDC2145584 (**4a**), CDC2290744 (**4b**), and CCDC2361752 (**4c**) Contain the Supplementary Crystallographic Data for This Paper. These Data Are Provided Free of Charge by the Cambridge Crystallographic Data Centre. Available online: https://www.ccdc.cam.ac.uk/ (accessed on 10 June 2024).
30. The Time-Dependence Density Functional Calculations Were Performed with Spartan'10, Wave Function, Irvine, CA. Available online: https://lab409.chem.ccu.edu.tw/~comchem100/Spartan10Manual.pdf (accessed on 10 June 2024).